

Supporting Information

A Cd-based MOF : Iodine Capture and Enhanced Efficiency of Perovskite Solar Cells

Yaxin Hou^{a,b}, Yang Liu^a, Juan Chai^{*a}

^aInstitute of Fire Safety Materials, School of Materials Science and Engineering, NingboTech University, Ningbo, 315100, P. R. China.

Email: chaijuan@nbt.edu.cn

^bMinhang Crosspoint Academy at Shanghai Wenqi Middle School, Shanghai, 200240, P. R. China.

Supporting Information

Table of Contents

1. Powder X-ray diffraction patterns of Cd-MOF. (Fig. S1)	S3
2. FT-IR spectrum of Cd-MOF. (Fig. S2)	S3
3. SEM image of Cd-MOF. (Fig. S3)	S4
4. TGA curve of Cd-MOF measured in air atmosphere. (Fig. S4)	S4
5. Binuclear $[\text{Cd}_2\text{O}_2(\text{L})_2(\text{COO})_2]$ cluster of Cd-MOF. (Fig. S5)	S5
6. 3D supramolecular structure of Cd-MOF. (Fig. S6)	S5
7. Calibration plot of iodine in a cyclohexane solution via a UV-vis spectrum. (Fig. S7)	S6
8. Adsorption amounts of MOF toward iodine in a cyclohexane solution of iodine when 40 mg of Cd-MOF is added. (Fig. S8)	S6
9. The image of the sample after I_2 adsorption. (Fig. S9)	S7
10. UV-vis spectra for temporal evolution of absorbance for the I_2 - released process in EtOH. (Fig. S10)	S7
11. Crystal and structure refinement data for Cd-MOF. (Table S1)	S8
12. Selected bond lengths [\AA] and angles [$^\circ$] for Cd-MOF. (Table S2)	S9
13. EIS measurements of PSCs without and with Cd-MOF treatment. (Fig. S11)	S9
14. Comparisons of device PCE between our PSCs and reported PSCs with MOF treatments (Table S3).	S10
15. Comparison of I_2 adsorption capacity of MOFs (Table S4).	S10-11

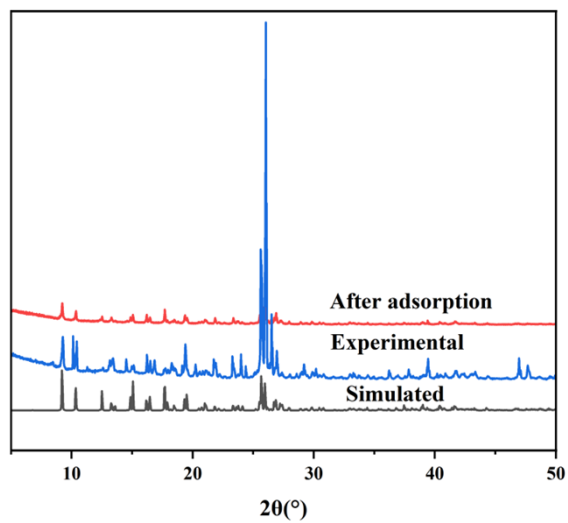


Fig. S1 Powder X-ray diffraction patterns of Cd-MOF.

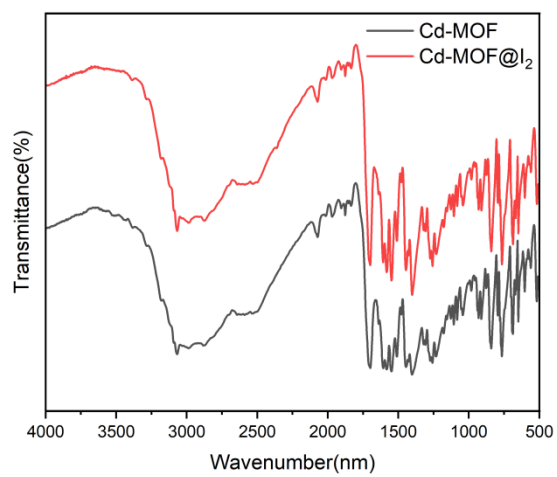


Fig. S2 FT-IR spectrum of Cd-MOF.



Fig. S3 SEM image of Cd-MOF.

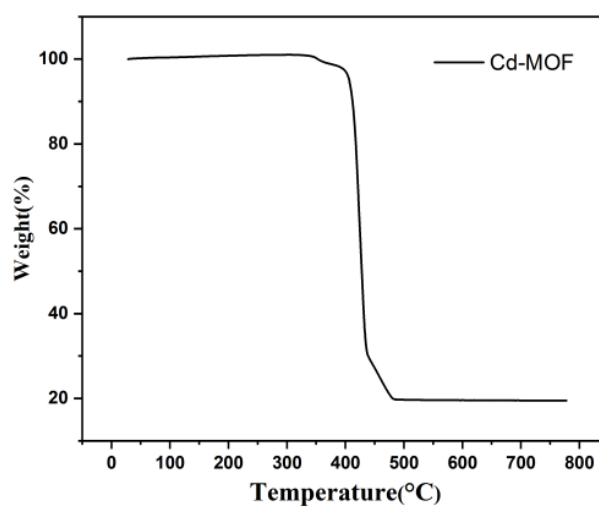


Fig. S4 TGA curve of Cd-MOF measured in air atmosphere.

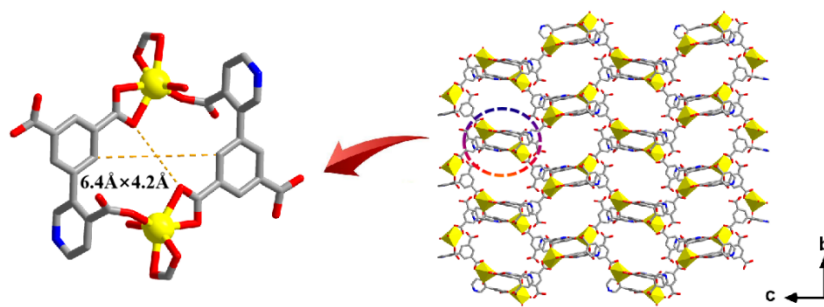


Fig. S5 Binuclear $[\text{Cd}_2\text{O}_2(\text{L})_2(\text{COO})_2]$ cluster of Cd-MOF .

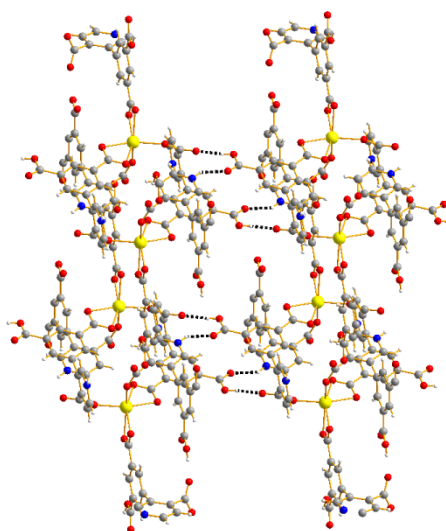


Fig. S6 hydrogen bonds of Cd-MOF.

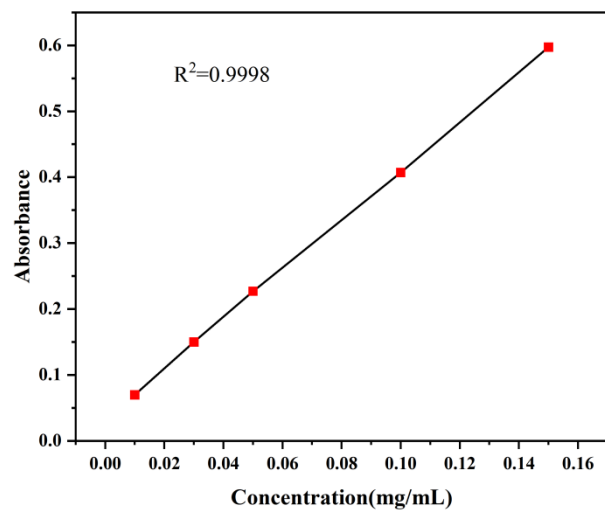


Fig. S7 Calibration plot of iodine in a cyclohexane solution via a UV-vis spectrum.

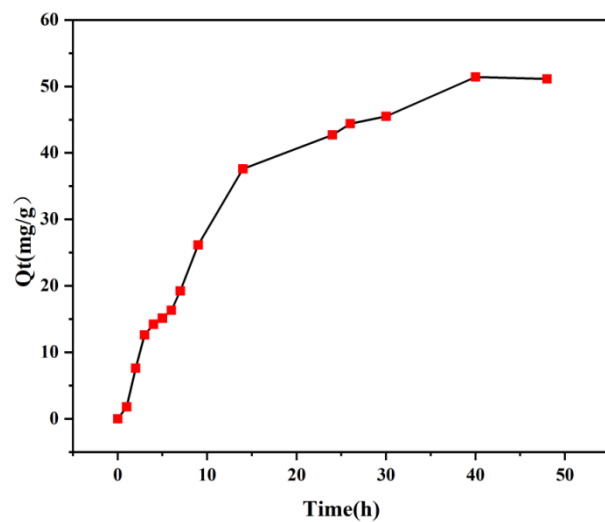


Fig. S8 Adsorption amounts of MOF toward iodine in a cyclohexane solution of iodine when 40 mg of Cd-MOF is added.

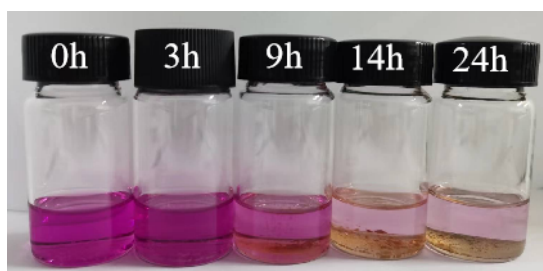


Fig. S9 The image of the sample after I₂ adsorption.

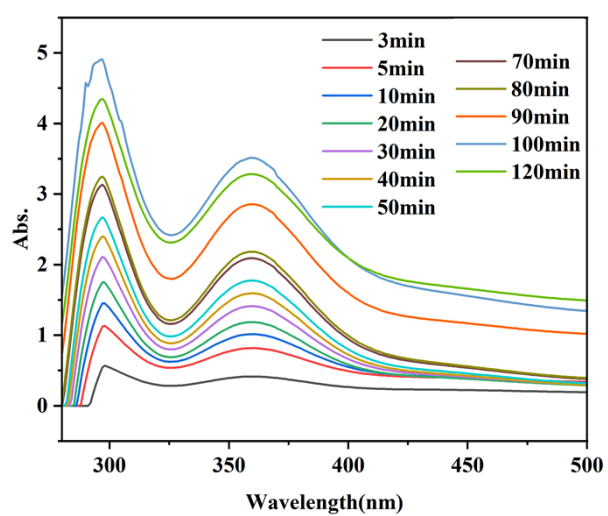


Fig. S10 UV-vis spectra for temporal evolution of absorbance for the I₂ -released process in EtOH.

Table S1 Crystal and structure refinement data for Cd-MOF

MOFs	Cd-MOF
chemical formula	$C_{28}H_{16}CdN_2O_{12}$
fw	684.83
cryst system	monoclinic
space group	$C2/c$
a/Å	13.8767(4)
b/Å	13.7096(4)
c/Å	26.8754(8)
α /deg	90
β /deg	103.797(3)
γ /deg	90
$V/\text{Å}^3$	4965.4
T/K	299
Z	8
$D_c/\text{g cm}^{-3}$	1.832
μ/mm^{-1}	0.957
F(000)	2736.0
	$-18 \leq h \leq 17$
index ranges	$-18 \leq k \leq 17$
	$-35 \leq l \leq 34$
R_{int}	0.0646
GOF on F^2	1.062
$R_1[I > 2\sigma(I)]$	0.0378
$wR_2[I > 2\sigma(I)]$	0.1033
CCDC No.	2371872

$$^a R_1 = \frac{\sum |F_o| - |F_c|}{\sum |F_o|}, \quad ^b wR_2 = \frac{\sum [w(F_o^2 - F_c^2)^2]}{\sum [w(F_o^2)^2]}^{1/2}$$

Table S2 Selected bond lengths [\AA] and angles [$^\circ$] for Cd-MOF

Cd(1)-O(10)	2.324(2)	Cd(1)-O(7)	2.217(2)
Cd(1)-O(5)	2.308(2)	Cd(1)-O(9)	2.333(2)
Cd(1)-O(1)	2.243(2)	Cd(1)-O(6)	2.361(2)
O(10)-Cd(1)-O(9)	56.27(8)	O(10)-Cd(1)-O(6)	102.33(9)
O(7)-Cd(1)-O(10)	148.84(8)	O(7)-Cd(1)-O(5)	88.11(8)
O(7)-Cd(1)-O(9)	94.10(8)	O(7)-Cd(1)-O(1)	95.19(8)
O(7)-Cd(1)-O(6)	105.25(9)	O(5)-Cd(1)-O(10)	95.42(8)
O(5)-Cd(1)-O(9)	114.26(8)	O(5)-Cd(1)-O(6)	56.18(8)
O(9)-Cd(1)-O(6)	157.44(9)	O(1)-Cd(1)-O(10)	98.93(8)
O(1)-Cd(1)-O(5)	145.72(8)	O(1)-Cd(1)-O(9)	99.57(9)
O(1)-Cd(1)-O(6)	90.26(8)		

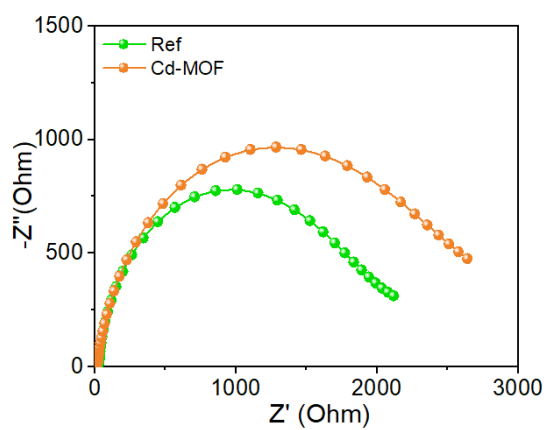
**Fig. S11** EIS measurements of PSCs without and with Cd-MOF treatment.

Table S3. Comparisons of device PCE between our PSCs and reported PSCs with MOF treatments.

PCE (%)	J_{sc} (mA/cm ²)	V_{oc} (V)	FF (%)	ref
23.71	25.16	1.179	79.90	Our work
18.10	22.1	1.11	73.9	1
12.0	23.04	0.93	60	2
22.16	23.71	1.14	82	3
20.24	22.85	1.12	79.1	4

Ref:

1. Y.-N. Zhang, B. Li, L. Fu, Q. Li, L.-W. Yin, *Electrochim. Acta*, 2020, **330**, 135280.
2. T.-H. Chang, C.-W. Kung, H.-W. Chen, T.-Y. Huang, S.-Y. Kao, H.-C. Lu, M.-H. Lee, K.M. Boopathi, C.-W. Chu, K.-C. Ho, *Adv. Mater.*, 2015, **27**, 7229-7235.
3. J. Dou, C. Zhu, H. Wang, Y. Han, S. Ma, X.X. Niu, N.X. Li, C.B. Shi, Z.W. Qiu, H.P. Zhou, Y. Bai, Q. Chen, *Adv. Mater.*, 2021, **33**, 2102947.
4. L.Y. Lou, L. Wan, Z.S. Wang, *ACS Appl. Mater. Interfaces*, 2023, **15**, 37059-37068.

Table S4 Comparison of I₂ adsorption capacity of MOFs

MOF material	Solution media	adsorption capacity (mg g ⁻¹)	Ref.
Cd-MOF	Cyclohexane	51.4	This work
IFMC-10	Hexane	40	1
Th-TATAB	Cyclohexane	75	2
{[Zn ₂ (α -bptc)(H ₂ O) ₄] \cdot pra} _n	Methanol	85	3
MIL-125-NH ₂ @chitosan	H ₂ O	19	4
[Cd ₃ (BTC) ₂ (TIB) ₂] _n	Hexane	160	5

Ref.:

1. L. Chen, K. Tan, Y.Q. Lan, S.L. Li, K.Z. Shao, Z. M. Su, *Chem. Commun.*, 2012, **48**, 5919-5921.
2. N. Zhang, L. X. Sun, Y. H. Xing, F. Y. Bai, *Cryst. Growth Des.*, 2019, **19**, 5686-5695.
3. S.S. Feng, Y.T. Bai, J.L. Zhu, L.P. Lu, M.L. Zhu, *Spectrochim. Acta, Part A*, 2018, **205**, 139-145.
4. M. El-Shahat, A.E. Abdelhamid, R.M. Abdelhameed, *Carbohydr. Polym.*, 2020, **231**, 115742.
5. Y. Rachuri, K.K. Bisht, B. Parmar, E. Suresh, *J. Solid State Chem.*, 2015, **223**, 23-31.